

Evaluating Power Loss and Performance Ratio of Hot-Spotted Photovoltaic Modules

Mahmoud Dhimish, *Member, IEEE*, Peter Mather, Violeta Holmes, *Member, IEEE*

Abstract—The impact of Photovoltaic (PV) hot-spots is assessed through the analysis of 2580 polycrystalline silicon PV modules distributed across the UK. PV hot-spots were categorized into eight different groups using the percentage of power loss (PLL). All hot-spots groups were modelled using the cumulative density function (CDF), state of art geographical mapping, and performance ratio (PR) analysis. Significantly, it was found that 92.15% of the PV modules affected by hot-spotted PV string are located in northern UK, were the effect of low temperature levels, heavy snow, and hoarfrost are more significant. Lastly, it was found that the distribution of PV modules affected by only one hot-spotted solar cell, are likely (82.41%) located in coastal locations. Hence, coastal locations expect to have lower risks for causing multiple hot-spotted solar cells in PV modules, compared to central and colder locations. The PR of all examined PV modules was analysed. It was evident that the mean PR is significantly reduced due to the existence of hot-spots in the PV modules. The least difference in the PR between healthy and hot-spotted PV modules is equal to -0.83%, whereas the most difference is calculated at -15.47%.

Index Terms—Photovoltaic; Solar Energy; Hot-Spots; CDF Modelling; Probability; Power Loss; PV Defects.

I. INTRODUCTION

HOT-SPOTTING is a reliability problem in Photovoltaic (PV) modules, this phenomena is well-identified when a mismatched solar cell heats up significantly and reduces the PV module output power [1]. PV hot-spots occur when a cell, or group of cells activates at reverse-bias, dissipating power instead of delivering it, and consequently operating at anomalous elevated temperature levels [2] and [3]. The hot-spots are also the main cause of accelerated PV ageing, and sometimes irreversible damage of entire PV panels [4].

There are a number of other reliability issues affecting PV modules such as PV module disconnection [5], faults associated with maximum power point tracking (MPPT) units [6] and [7], PV micro cracks [8], and fluctuations in the wind speed and humidity variations [9]. All of these factors affect the PV module output power performance, thus decreasing

annual energy production. However, this article addresses the impact of hot-spotting in PV modules.

PV hot-spots can easily be detected using infrared (IR) inspection, which has become a common practice in current PV application as presented in [10]. However, the impact of hot-spots on the operation and performance of PV modules have significantly been often addressed, which helps us to explain why there is a lack of accepted approaches which deal with hot-spotting as well as specific criterion referring to the acceptance or rejection of affected PV module in commercial frameworks.

In the past, and still in general practice, hot-spotting effects were usually mitigated by the adoption of bypass diodes which are parallelized with the PV modules, with the target to limit the maximum reverse voltage across the hot-spotted or shaded solar cells, this use of bypass diodes increases the overall short circuit current and the open circuit voltage [11] – [13]. However, this method is not ideal since it requires additional cost and can be even detrimental in terms of power dissipation caused by the additional bypass diodes as discussed by Manganiello *et al.* [14].

Most recently, a distributive MPPT method suggested by Coppola *et al.* [15] and Olalla *et al.* [16], to mitigate hot-spots in PV modules, yielded an approximate reduction up to 20 °C for small and medium hot-spotting areas. On the other hand, Kim and Krein [17] show the “inadequateness” of the standard bypass diodes, by the insertion of a series-connected switch are suited to interrupt the current flow during bypass activation process. However, this solution requires a relatively complex electronic board design that needs devised power supply and appropriate control logic for activating the hot spot protection device.

In 2018, two hot-spot mitigation techniques developed by Dhimish *et al.* [18]. Based on MOSFETs connected to the PV module in order to switch ON/OFF the hot-spotted PV solar string. The proposed techniques are proved reliable, but do not contain any modelling or statistical analysis for the overall impact of PV hot-spots on the output power performance.

The main motivation of this work, firstly, to analyse the impact of hot-spots on the performance of PV modules. The analysis not only considers local PV modules at specific geographical locations, but also a wide range of PV modules distributed across the UK. Therefore, a total of 2580 examined hot-spotted PV modules. This will ensure that the analysis is based on PV modules affected by various environmental conditions such as fluctuations in the wind, irradiance, temperature, and humidity levels. Secondly, propose a suitable modelling technique based on cumulative density function

Manuscript received 30th July 2018; revised 27th September 2018, and 21st October 2018.

Mahmoud Dhimish*, Peter Mather, and Violeta Holmes are with the Department of Engineering and Technology, Photovoltaic Laboratory, University of Huddersfield, Huddersfield, HD1 3DH (*Corresponding author (M. Dhimish): email: Mahmoud.dhimish@gmail.com)

(CDF) function in order to categories PV hot-spots into various groups.

As far as the authors are concerned, there is no other probabilistic or statistical models describing the impact of the hot-spots on the performance of PV modules based on large scale PV datasets (i.e. >2500 hot-spotted PV modules data).

II. METHODOLOGY

A. Examined PV modules

The distributed PV installations data were collected via Solar UK database system, which has the PV modules and strings output voltage, current, and power.

The geographical map presenting the distribution of the PV installations across the UK (only in England, Wales, and Scotland) are shown in Fig. 1. The total inspected PV modules within all examined PV installations are equal to 8340, with the PV technology being Polycrystalline Silicon (Poly-Si).

The majority of the PV modules were installed from 2005 to 2007, the PV modules were supplied by a combination of homeowners and commercial scale PV installations between 1.1 and 50 kWp with a wide range of orientation and tilt angles.

The collection of the data was taken on-site from various PV companies, alongside multiple current-voltage (I-V) and power-voltage (P-V) curve tracer, these instruments are subject to different errors, accuracy, and tolerance rates. Therefore, the data collected from the PV modules were subjected to demanding checks and validation in order to remove and isolate as much inaccurate data as possible. The standard set of filters employed prior to data analysis and investigation stage are as follows:

- The PV modules I-V and P-V curves were captured under same environmental conditions including solar irradiance level, ambient temperature, humidity, and shading factors.
- Take into account only PV modules within the UK, since the database contains multiple PV systems installed in wide range of European countries.



Fig. 1. Geographical map for the PV sites locations used in the analysis

- Use only systems with a tilt angle from 30° to 60° , and orientation between -30° to $+30^\circ$.
- Use only PV systems with accessible PV modules data; thus it is possible to compare between hot-spotted and adjacent free hot-spotted PV modules.
- Accuracy of instruments and sensors are within the range of $99.7\% \geq \text{accuracy} (\eta) \geq 95\%$. No issues with MPPT units were determined; they are highly efficient. The major sources of errors could be the measurement and correction of temperature and irradiance (measurement of the healthy and hot-spotted PV modules on different time).

After the interpretation of the selective requirements have been carried out, 6159 PV modules remain (out of 8340). The PV modules is shown in Fig. 2. The number of PV modules which did not contain hot-spots is equal to 3579, which presents 58% of the total inspected PV modules. Whereas the probability of the total PV modules contains hot-spotted PV cells are equal to 42%.

Based upon the available datasets, the hot-spotted PV solar cells were categorized into five groups, it was found that total PV modules affected by each category is equal to:

- 1 hot-spotted solar cell in a PV module: 1058
- 2 hot-spotted solar cells in a PV module: 491
- 3 hot-spotted solar cells in a PV module: 542
- 4 hot-spotted solar cell in a PV module: 283
- ≥ 5 hot-spotted solar cell in a PV module: 155

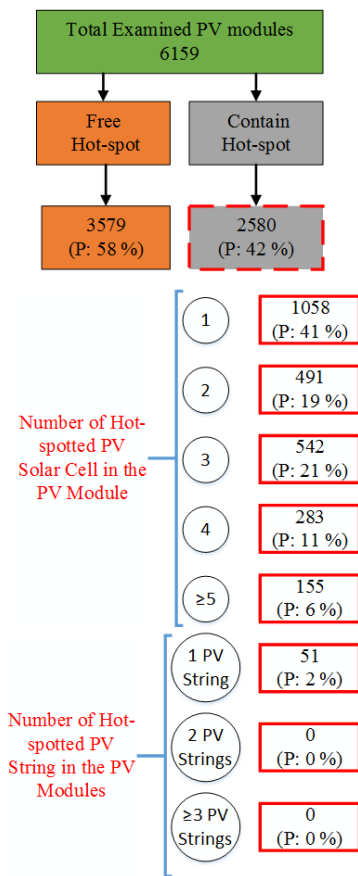


Fig. 2. Hot-spots probability of occurrence among all tested PV modules

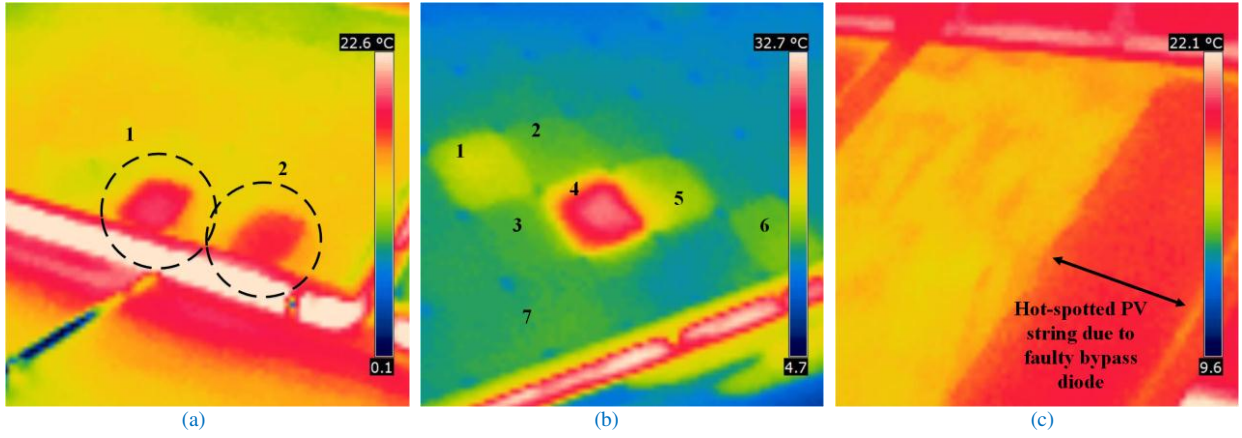


Fig. 3. Examples for three different types of hot-spots affecting PV modules. (a) Two hot-spots, (b) >5 hot-spots, (c) Hot-spotted PV string

Additionally, it was found that fifty-one PV modules out of 2580 contain one hot-spotted PV string. Interestingly, none of the PV modules had two or more hot-spotted PV strings.

Fig. 3 shows an example of three different hot-spots categories, which were identified using a FLIR thermal imaging camera [19]. Fig. 3(a) shows two solar cell affected by a hot-spot, whereas Figs. 3(b) and 3(c) present multiple (>5) hot-spotted solar cells, and one hot-spotted PV string in a PV module respectively.

Initial investigations demonstrated a correlation between the output power losses from each hot-spots category, but, in order to draw relevant outcomes and novel conclusions, each of the inspected category was modelled independently.

B. Percentage of Power Loss (PPL) technique

In order to investigate the power losses in the PV modules affected by hot-spots, and since the PV modules have different output peak power, the percentage of power loss (PPL) technique was used.

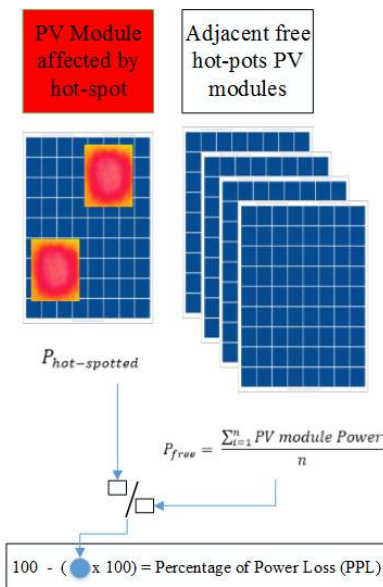


Fig. 4. Percentage of power loss (PPL) estimation for hot-spotted and free hot-spotted PV modules

Initially, the output power from the PV module affected by hot-spots ($P_{hot-spotted}$) is measured, and then divided by the average output power from adjacent free hot-spotted PV modules. The adjacent average power is calculated using (1). Fig. 4, briefly explains the assessment of the PPL technique.

The calculations of the PPL including the measured and theoretical voltage and current are taken under 1-Sun condition available in the collected database. In fact, we have not used any mathematical expressions/equations to correct the collected data, since irradiance and temperature sensors are available in the examined PV sites.

$$P_{free} = \frac{\sum_{i=1}^n PV \text{ module Power}}{n} \quad (1)$$

III. RESULTS

A. PPL and CDF modelling

The evaluation of the data driven by the observed hot-spots and the distribution over histogram profiles are shown in Fig. 5. The histograms contain the PPL values for all the defined categories of the hot-spotted PV modules, as well as the frequency of the PPL at certain levels.

According to Fig. 5, it is evident that the PV modules affected by one hot-spotted solar cell have the least drop in the PPL as shown in Fig. 5(a), the average of the PPL is equal to 0.95% over a sample size of 1058 PV modules.

The increase in the number of hot-spotted solar cell would increase the percentage of the power loss; for example, Fig. 5(b) shows that the average PPL is equal to 2.0% for PV modules affected by two hot-spotted solar cells. These results are evaluated over a sample size of 491 PV modules.

The average percentage of the power loss for all other hot-spots categories are summarized follows:

- Three hot-spots in a PV module is equal to 2.7%
- Four hot-spots in a PV module is equal to 4.0%
- ≥ 5 hot-spots in a PV module is equal to 11%
- One PV string in a PV module is equal to 19%

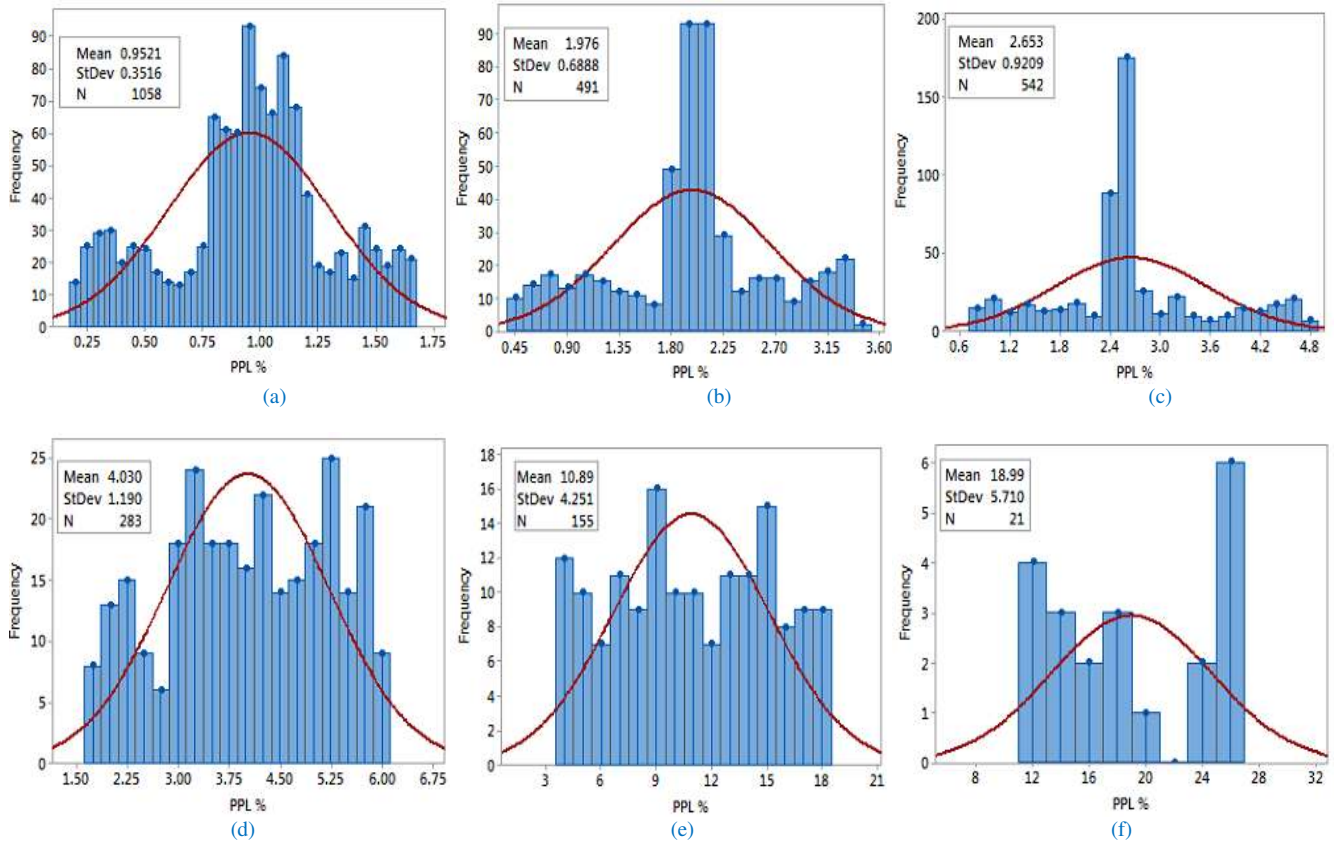


Fig. 5. Histogram for the PPL vs. frequency of the samples. (a) 1 hot-spotted solar cell, (b) 2 hot-spotted solar cells, (c) 3 hot-spotted solar cells, (d) 4 hot-spotted solar cells, (e) ≥ 5 hot-spotted solar cells, (f) Hot-spotted PV string in a PV module

Interestingly, the increase number of hot-spots in PV modules, it is more likely to have greater drop in output peak power. On the other hand, the PV modules with a complete hot-spotted PV string is caused due to faulty bypass diodes. Therefore, there is more chance to have less output power produced by these particular PV modules, since bypass diodes overcome the issue of the partial shading conditions which normally PV modules suffer from.

In addition, it is worth remembering that all data presented in Fig. 5 are subject to various errors such as the PV system sensors accuracy rate, data collection accuracy, and some other environmental factors, in which the data collected from the observed PV modules were subjected to demanding checks and validation in order to remove and isolate as much inaccurate data as possible.

The data shown in Fig. 5 could additionally be used to implement a relevant theoretical model to predict the hot-spots in other PV modules. Thus, it is ideally conceivable to inspect PV modules and predict the number of hot-spotted solar cells. This feature has been implemented using the cumulative density function (CDF) modelling technique [20] and [21], which will be describe next.

The provision of probabilistic and error analysis projections is the major improvements which many researchers worldwide relies on to extensively prove/disapprove the chance of an action to accrue [22]. Probabilistic projections assign a probability to different possible weather conditions outcomes, recognize that: (i) we cannot give a single answer, and (ii)

giving range of possible outcomes is better, and can help with marking a robust adaption for the results decisions. However, a range of possible outcomes will limit the findings within a range of thresholds.

According to the previously discussed data shown in Fig. 5, the PPL for PV modules affected by 1, 2, 3, and 4 hot-spotted solar cells are relatively equivalent, where the average PPL varies between 1.0% and 4.0%. However, the PPL for the PV modules affected by either ≥ 5 hot-spotted solar cells or one hot-spotted PV string almost between 5.0% and 30%. In that case, we have alienated the CDF modelling into two main profiles, principally shown in Fig. 6, where x-axis presents the PPL and the percentage of occurrence corresponds to y-axis.

CDF plots for the PV modules affected by 1 to 4 hot-spotted solar cells are shown in Fig. 6(a). As an example, the first line (blue) is the CDF model for the PV modules affected by one hot-spotted solar cell, 90% of the examined PV modules have a percentage of power loss below 1.4%, whereas 10% has PPL below 0.5%. Therefore, the CDF models present the percentage of the PV modules affected by various hot-spot conditions.

According to Fig. 6(a), 10% and 90% of the total observed PV modules have a percentage of power loss equals to the following:

- PPL threshold for one hot-spot: 0.5% – 1.4%
- PPL threshold for two hot-spots: 1.1% – 2.9%
- PPL threshold for three hot-spots: 1.5% – 3.8%
- PPL threshold for four hot-spots: 2.5% – 5.6%

The CDF plots for the PV modules affected by either ≥ 5 hot-spotted solar cells or one hot-spotted PV string are shown in Fig. 6(b), and illustrates that the PPL thresholds between 10% and 90% are equal to:

- ≥ 5 hot-spots in a PV module: 5.4% – 16.3%
- One PV string in a PV module: 11.7% – 26.3%

As a result, due to the failure of the bypass diodes, the power loss of a PV modules is from 11.7% to 26.3%. The main reason for this variations in the output power loss is due to fluctuations in the partial shading conditions/scenarios affecting the defective PV module. Thus, low percentages of partial shading conditions result in reduced output power loss.

In order to validate this result, we have examined the PV module shown in Fig. 3(c) under three different shading conditions, whilst the PV module temperature is 25 °C, and irradiance of 1000 W/m². This PV modules is affected by a hot-spotted PV string caused by a defective bypass diode. Fig. 7(a) shows the Power-Voltage (P-V) curve for healthy vs. defective PV module under low partial shading condition (15%). The measured PPL is equal to 13.36%, whereas the PPL is equal to 17.03% and 20.96% at 30% and 60% partial shading conditions, respectively.

The obtained results of this experiment proves that shading conditions play viral role in increasing/decreasing the amount of PPL of the hot-spotted PV modules. Furthermore, this experiment confirms that the measured PPL (13.36% - 20.96%) shown in Fig. 7 lies within the PPL thresholds (11.7% - 26.3%) obtained using the analysis of 51 hot-spotted PV strings shown in Fig. 5.

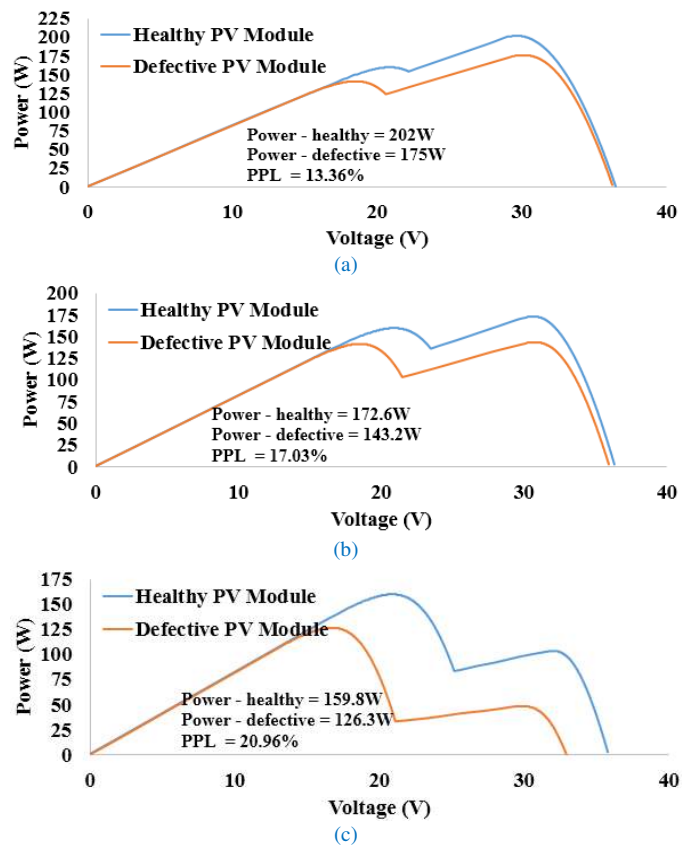


Fig. 7. Power-Voltage curve measured at different partial shading condition for defective bypass diode scenario. (a) 15% shading condition, (b) 30% shading condition, (c) 60% shading condition

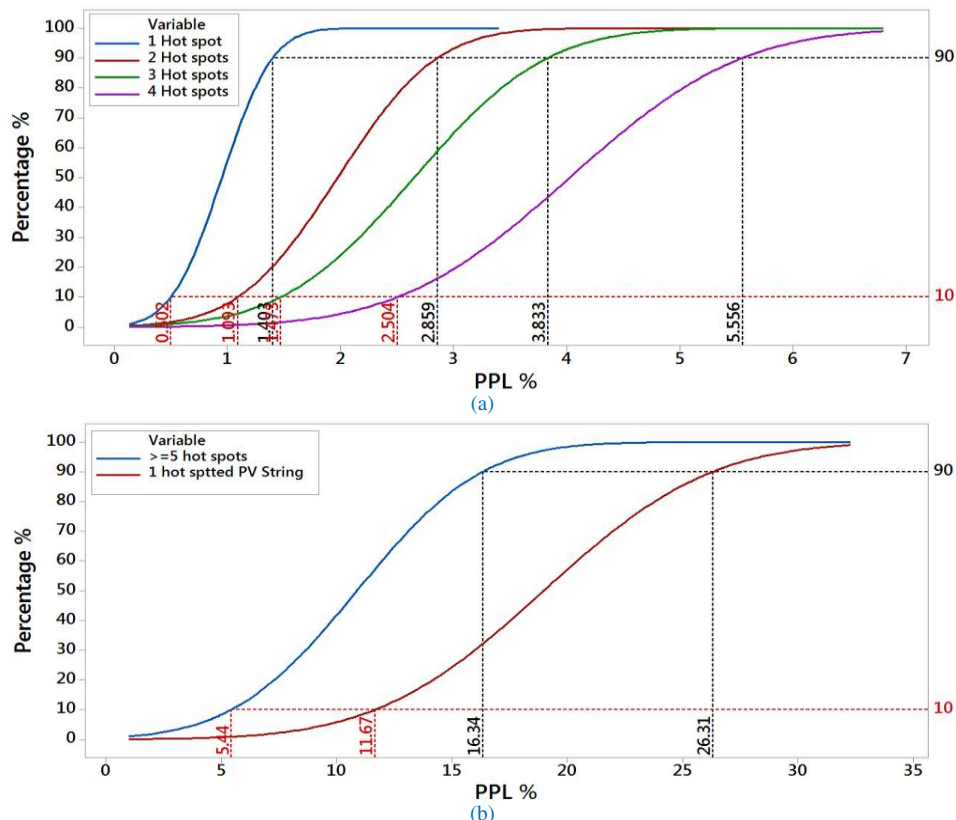


Fig. 6. Cumulative density function (CDF) models. (a) CDF model for PV modules affected by 1 to 4 hot-spotted solar cells, (b) CDF model for PV modules affected by either ≥ 5 hot-spotted solar cells or one hot-spotted PV string in a PV module

B. State-of-Art Geographical distribution of the examined hot-spotted PV modules

In this section, a remarkable finding on the distribution of the examined hot-spotted PV modules will be demonstrated using a geographical representation. Here, we include two substantial observations based upon the hot-spotted PV modules distribution, and are summarized as follows:

First Observation: 92.15% (47 out of 51) PV modules affected by one hot-spotted PV string are located in the north of the UK as shown in Fig. 8(a). This location has the lowest temperature records as well as solar irradiance among all other UK districts. The hot-spotted PV strings are produced due to the failure in the bypass diodes of the affected PV module, as a result, increases the PV string temperature. Two examples are shown in Figs. 8(b) and 8(c), where the increase in the PV string temperature is equal to 7.9 °C and 9.1 °C. Hence, cold locations, more specifically, northern UK sites, have higher

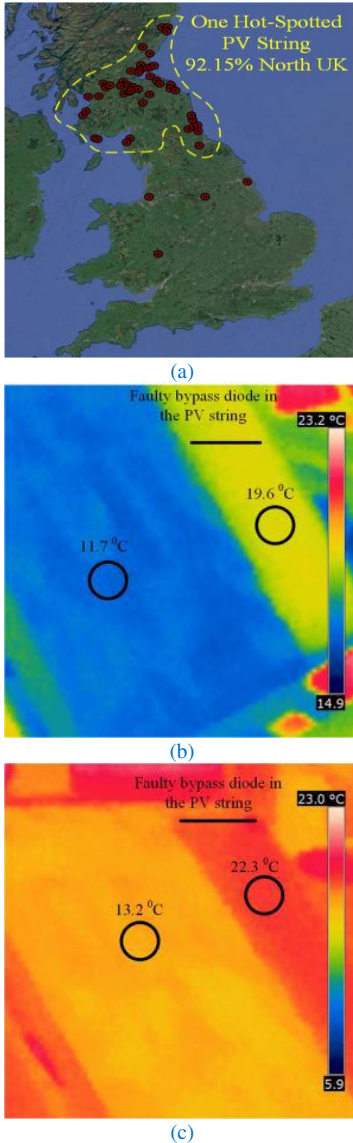


Fig. 8. (a) Geographical distribution for PV modules affected by one hot-spotted PV string (92.15% north UK), (b) Faulty bypass diode in a PV string increasing the temperature of the string by 7.9 °C, (c) Faulty bypass diode in a PV string increasing the temperature string by 9.1 °C

risks of bypass diode failure due to weather conditions such as heavy snow, hoarfrost, and low temperature levels, therefore, increasing the risks to cause hot-spotting PV strings.

Second Observation: Another noteworthy result is shown in Fig. 9. This figure includes the distribution of the PV modules affected by one hot-spotted solar cell. Interestingly, 82.41% (872 out of 1058) PV modules affected by this type of hot-spotting are located in coastal locations. These sites are typically affected by high wind speed (ultimately cooling the PV modules [23]), rapid deviations in humidity levels (lower humidity yield better performance of PV modules [24]), and lower temperature records compared to central UK. Therefore, coastal locations expect to have lower risks for causing multiple hot-spotted solar cells in PV modules, compared to central and cold sites.

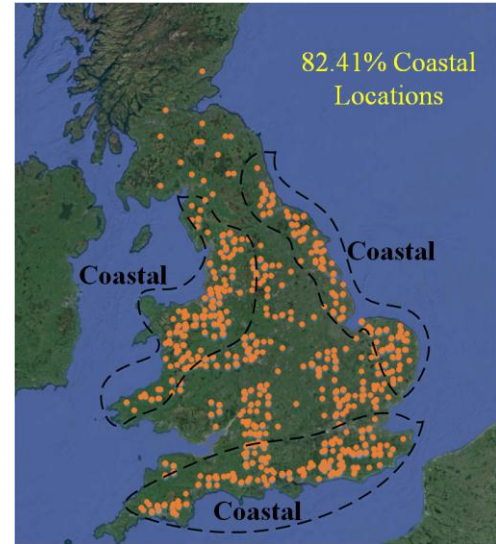


Fig. 9. Geographical distribution for PV modules affected by one hot-spotted solar cell (82.41% coastal locations)

C. Photovoltaic Modules Performance Ratio Analysis

Performance ratio (PR) is a widely used metric for comparing relative performance of PV installations whose design, technology, capacity, and location differ [25] and [26]. The PR is calculated using using (2).

$$PR = \frac{\eta_{measured}}{\eta_{theoretical}} = \frac{\frac{E}{G}}{\eta_{theoretical}} \quad (2)$$

where $\eta_{measured}$ and $\eta_{theoretical}$ are the actual measured efficiency and theoretical output efficiency of the examined PV installations, E is the output energy of the PV system (kWh), and G is the solar irradiance incident in the plant of the PV array (kWh).

The normal distribution of the PR for all examined PV modules is shown in Figs. 10 and 11. We have distributed the analysis of the PR over two different periods, from 2009 – 2012 and from 2013 to 2017 (last 5 years of PV operation). The shape of the output results is categorized by the normal distribution function, whereas the total number of PV modules are shown earlier in Fig. 2.

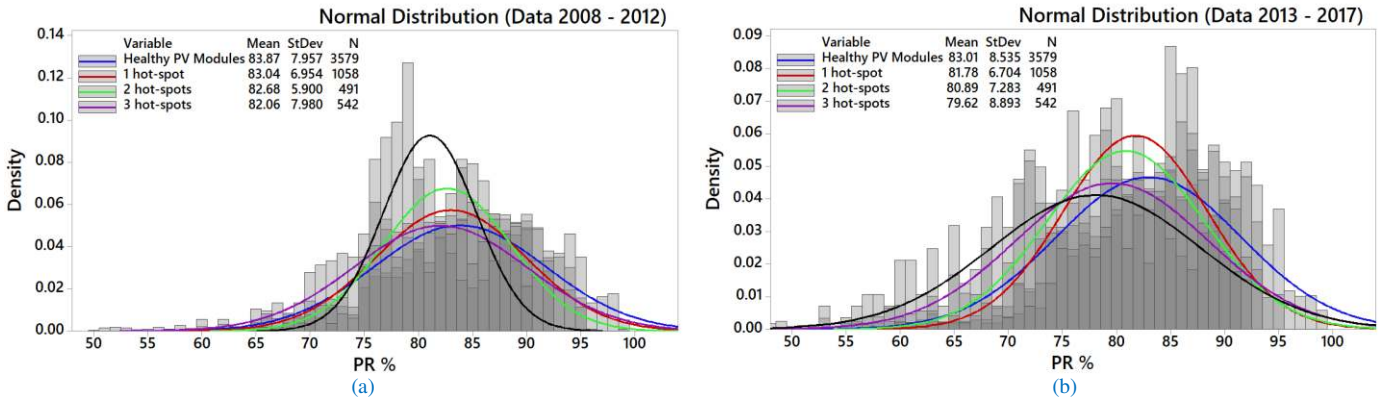


Fig. 10. Histogram of the yearly performance ratio and its normal distribution curve over a period of 10 years – healthy, 1 hot-spotted, 2 hot-spotted, and 3 hot-spotted photovoltaic modules. (a) PR from 2008 to 2012, (b) PR from 2013 to 2017

According to Fig. 10, both histograms present the PR for the examined PV modules affected by 1, 2, and 3 hot-spotted solar cells and compared with the healthy PV modules.

From 2008 to 2012, the mean PR of the healthy PV modules is equal to 83.87% with a standard deviation (StDev) of 7.95%. As shown in Fig. 10(a), there is a reduction in the PR of -0.83%, -1.19%, and -1.81% for the PV modules affected by 1, 2, and 3 hot-spotted PV cells respectively.

As presented in Fig. 10(b), the mean PR of the healthy PV modules is equal to 83.01%, reduced by -0.86% compared to the first five years of operation: $83.87\% - 83.01\% = 0.86\%$. Nevertheless, there is a higher rate of reduction in the PR for the hot-spotted PV modules, the reduction is as follows:

- 1 hot-spotted PV modules: -1.25%
- 2 hot-spotted PV modules: -2.14%
- 3 hot-spotted PV modules: -3.41%

The comparison between the PR of the healthy PV modules and the PV modules affected by either ≥ 5 hot-spotted PV cells, or one hot-spotted PV string are shown in Fig. 11. The results of the mean PR from 2008 to 2012 are summarized as follows:

- Healthy PV modules: 83.87%
- ≥ 5 hot-spotted solar cells: 74.10%
- Hot-spotted PV string: 71.59%

Therefore, the reduction in the PR of the hot-spotted PV modules is equal to -9.77% and -12.28% respectively. Compared to healthy PV modules, there is higher drop in the

PR from 2013 to 2017 for the hot-spotted PV modules (shown in Fig. 11(b)). This reduction is equal to -12.76% for the PV modules affected by ≥ 5 hot-spotted PV cells, and -15.47% for the PV modules affected by one hot-spotted PV string.

This section confirms that the PV modules affected by hot-spotting phenomenon is likely to affect the PPL and PR alike. Furthermore, the reliability and yield energy of the PV system will significantly be affected.

D. Recommendations

As per results obtained in this research, the authors would suggest the following recommendations:

- In cold regions, practically PV modules affected by heavy snow, hoarfrost, and low temperature levels, it is recommended to frequently check the performance for the PV modules, since in these locations PV modules are likely to suffer from hot-spotting and other mismatch conditions such broken glass.
- PV modules affected by multiple hot-spotted PV cells or defective bypass diodes have to be replaced, since these modules significantly reduce the reliability and the yield energy of the PV installations.
- PV modules installed in costal locations are less likely to be affected by the hot-spotting phenomenon.
- PV research community and solar energy industry have to start investigating the impact of PV hot-spotting on the accuracy of current maximum power point tracking (MMPT) units available in the market.

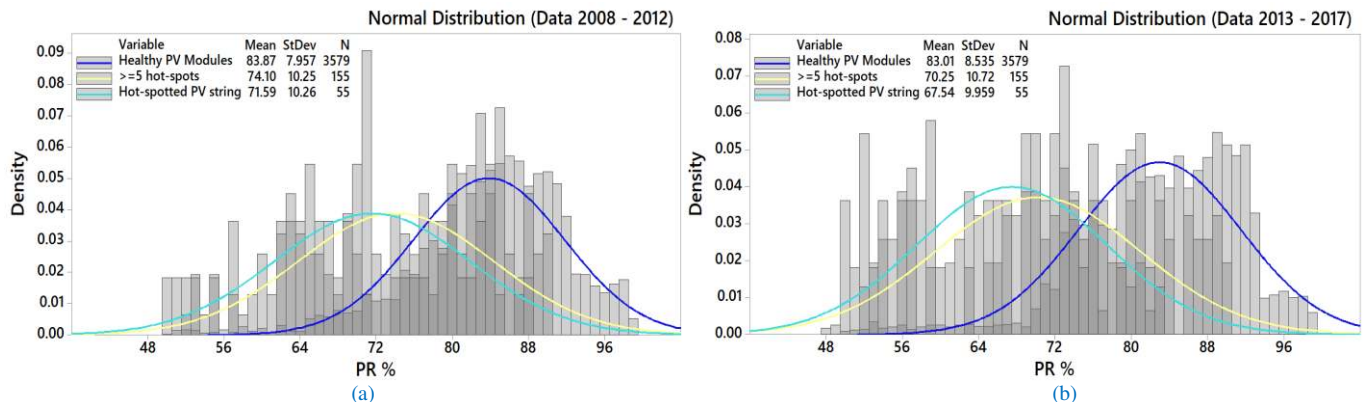


Fig. 11. Histogram of the yearly performance ratio and its normal distribution curve over a period of 10 years – healthy PV module, ≥ 5 hot-spotted PV module, and PV module with hot-spotted PV string. (a) PR from 2008 to 2012, (b) PR from 2013 to 2017

IV. CONCLUSION

Hot-spotting is a reliability problem affecting PV modules worldwide. High PV solar cell temperature due to hot-spotting can damage the cell, and lead to secondary breakdown. Therefore, in this paper the evaluation of the percentage of power loss (PLL) due to hot-spots affecting PV module is assessed.

It was found that increasing number of hot-spotted solar cells in a PV module, would likely increase its output power loss through the estimation of the PPL. Another remarkable result found that 92.15% of the PV modules affected by hot-spotted PV string are located in northern UK, relatively affected by low temperature levels, heavy snow, and hoarfrost. Furthermore, it was found that the distribution of PV modules affected by only one hot-spotted solar cell, are likely (82.41%) located in coastal locations.

Lastly, the performance ratio (PR) of all examined PV modules was analyzed. It was evident that the mean PR is significantly reduced due to the existence of hot-spots in the PV modules. The least difference in the PR between healthy and hot-spotted PV modules is equal to -0.83%, whereas the most difference is calculated at -15.47%.

REFERENCES

- [1] T. Ghanbari, "Permanent partial shading detection for protection of photovoltaic panels against hot spotting," in *IET Renewable Energy Generation*, vol. 11, no. 1, pp. 123-131, 2017, doi: [10.1049/iet-rpg.2016.0294](https://doi.org/10.1049/iet-rpg.2016.0294).
- [2] M. Dhimish, V. Holmes, P. Mather, and M. Sibley, "Novel hot spot mitigation technique to enhance photovoltaic solar panels output power performance," in *Solar Energy Materials and Solar Cells*, vol. 179, pp. 72-79, June 2018, doi: [10.1016/j.solmat.2018.02.019](https://doi.org/10.1016/j.solmat.2018.02.019).
- [3] E. Moon, D. Blaauw and J. D. Phillips, "Subcutaneous Photovoltaic Infrared Energy Harvesting for Bio-implantable Devices," in *IEEE Transactions on Electron Devices*, vol. 64, no. 5, pp. 2432-2437, May 2017, doi: [10.1109/TED.2017.2681694](https://doi.org/10.1109/TED.2017.2681694).
- [4] N. J. Western, I. Perez-Wurfl, S. R. Wenham and S. P. Bremner, "Point-Contacting by Localized Dielectric Breakdown With Breakdown Fields Described by the Weibull Distribution," in *IEEE Transactions on Electron Devices*, vol. 62, no. 6, pp. 1826-1830, June 2015, doi: [10.1109/TED.2015.2423292](https://doi.org/10.1109/TED.2015.2423292).
- [5] H. S. Sahu and S. K. Nayak, "Extraction of Maximum Power From a PV Array Under Nonuniform Irradiation Conditions," in *IEEE Transactions on Electron Devices*, vol. 63, no. 12, pp. 4825-4831, Dec. 2016, doi: [10.1109/TED.2016.2616580](https://doi.org/10.1109/TED.2016.2616580).
- [6] M. Dhimish, V. Holmes, B. Mehrdadi and M. Dales, "Simultaneous fault detection algorithm for grid-connected photovoltaic plants," in *IET Renewable Power Generation*, vol. 11, no. 12, pp. 1565-1575, 2017, doi: [10.1049/iet-rpg.2017.0129](https://doi.org/10.1049/iet-rpg.2017.0129).
- [7] Z. Yi and A. H. Etemadi, "Fault Detection for Photovoltaic Systems Based on Multi-Resolution Signal Decomposition and Fuzzy Inference Systems," in *IEEE Transactions on Smart Grid*, vol. 8, no. 3, pp. 1274-1283, May 2017, doi: [10.1109/TSG.2016.2587244](https://doi.org/10.1109/TSG.2016.2587244).
- [8] M. Dhimish, V. Holmes, B. Mehrdadi, and M. Dales, "Development of 3D graph-based model to examine photovoltaic micro cracks," in *Journal of Science: Advanced Materials and Devices*, vol. 3, no. 3, pp. 380-388, 2018, doi: [10.1016/j.jsamd.2018.07.004](https://doi.org/10.1016/j.jsamd.2018.07.004).
- [9] N. G. Dhere, N. S. Shiradkar and E. Schneller, "Evolution of Leakage Current Paths in MC-Si PV Modules From Leading Manufacturers Undergoing High-Voltage Bias Testing," in *IEEE Journal of Photovoltaics*, vol. 4, no. 2, pp. 654-658, March 2014, doi: [10.1109/JPHOTOV.2013.2294764](https://doi.org/10.1109/JPHOTOV.2013.2294764).
- [10] T. Liao, Z. Yang, Q. Dong, X. Chen and J. Chen, "Performance Evaluation and Parametric Optimum Choice Criteria of a Near-Field Thermophotovoltaic Cell," in *IEEE Transactions on Electron Devices*, vol. 64, no. 10, pp. 4144-4148, Oct. 2017, doi: [10.1109/TED.2017.2731789](https://doi.org/10.1109/TED.2017.2731789).
- [11] W. L. Chen and C. T. Tsai, "Optimal Balancing Control for Tracking Theoretical Global MPP of Series PV Modules Subject to Partial Shading," in *IEEE Transactions on Industrial Electronics*, vol. 62, no. 8, pp. 4837-4848, Aug. 2015, doi: [10.1109/TIE.2015.2400414](https://doi.org/10.1109/TIE.2015.2400414).
- [12] F. G. Della Corte, G. De Martino, F. Pezzimenti, G. Adinolfi and G. Graditi, "Numerical Simulation Study of a Low Breakdown Voltage 4H-SiC MOSFET for Photovoltaic Module-Level Applications," in *IEEE Transactions on Electron Devices*, vol. 65, no. 8, pp. 3352-3360, Aug. 2018, doi: [10.1109/TED.2018.2848664](https://doi.org/10.1109/TED.2018.2848664).
- [13] M. Dhimish, V. Holmes, B. Mehrdadi, M. Dales, and P. Mather, "PV output power enhancement using two mitigation techniques for hot spots and partially shaded solar cells," in *Electric Power Systems Research*, vol. 158, pp. 15-25, 2018, doi: [10.1016/j.epr.2018.01.002](https://doi.org/10.1016/j.epr.2018.01.002).
- [14] P. Manganiello, M. Balato and M. Vitelli, "A Survey on Mismatching and Aging of PV Modules: The Closed Loop," in *IEEE Transactions on Industrial Electronics*, vol. 62, no. 11, pp. 7276-7286, Nov. 2015, doi: [10.1109/TIE.2015.2418731](https://doi.org/10.1109/TIE.2015.2418731).
- [15] M. Coppola, S. Daliento, P. Guerriero, D. Lauria and E. Napoli, "On the design and the control of a coupled-inductors boost dc-ac converter for an individual PV panel," *International Symposium on Power Electronics Power Electronics, Electrical Drives, Automation and Motion*, Sorrento, 2012, pp. 1154-1159, doi: [10.1109/SPEEDAM.2012.6264548](https://doi.org/10.1109/SPEEDAM.2012.6264548).
- [16] C. Olalla, Md. Hasan, C. Deline, and D. Maksimovic, "Mitigation of Hot-Spots in Photovoltaic Systems Using Distributed Power Electronics," in *Energies*, vol. 11, no. 4, pp. 726, 2018, doi: [10.3390/en11040726](https://doi.org/10.3390/en11040726).
- [17] K. A. Kim and P. T. Krein, "Reexamination of Photovoltaic Hot Spotting to Show Inadequacy of the Bypass Diode," in *IEEE Journal of Photovoltaics*, vol. 5, no. 5, pp. 1435-1441, Sept. 2015, doi: [10.1109/JPHOTOV.2015.2444091](https://doi.org/10.1109/JPHOTOV.2015.2444091).
- [18] M. Dhimish, V. Holmes, B. Mehrdadi, M. Dales, and P. Mather, "Output-Power Enhancement for Hot Spotted Polycrystalline Photovoltaic Solar Cells," in *IEEE Transactions on Device and Materials Reliability*, vol. 18, no. 1, pp. 37-45, March 2018, doi: [10.1109/TDMR.2017.2780224](https://doi.org/10.1109/TDMR.2017.2780224).
- [19] W. S. M. Brooks, D. A. Lamb and S. J. C. Irvine, "IR Reflectance Imaging for Crystalline Si Solar Cell Crack Detection," in *IEEE Journal of Photovoltaics*, vol. 5, no. 5, pp. 1271-1275, Sept. 2015, doi: [10.1109/JPHOTOV.2015.2438636](https://doi.org/10.1109/JPHOTOV.2015.2438636).
- [20] X. Zhu and N. Balakrishnan, "Exact Inference for Laplace Quantile, Reliability, and Cumulative Hazard Functions Based on Type-II Censored Data," in *IEEE Transactions on Reliability*, vol. 65, no. 1, pp. 164-178, March 2016, doi: [10.1109/TR.2015.2451617](https://doi.org/10.1109/TR.2015.2451617).
- [21] H. Wang, M. Liserre and F. Blaabjerg, "Toward Reliable Power Electronics: Challenges, Design Tools, and Opportunities," in *IEEE Industrial Electronics Magazine*, vol. 7, no. 2, pp. 17-26, June 2013, doi: [10.1109/MIE.2013.2252958](https://doi.org/10.1109/MIE.2013.2252958).
- [22] S. V. Amari, H. Pham and R. B. Misra, "Reliability Characteristics of \$k\$-out-of- n Warm Standby Systems," in *IEEE Transactions on Reliability*, vol. 61, no. 4, pp. 1007-1018, Dec. 2012, doi: [10.1109/TR.2012.2220891](https://doi.org/10.1109/TR.2012.2220891).
- [23] J. Wong, R. Sridharan and V. Shanmugam, "Quantifying edge and peripheral recombination losses in industrial silicon solar cells," in *IEEE Transactions on Electron Devices*, vol. 62, no. 11, pp. 3750-3755, Nov. 2015, doi: [10.1109/TED.2015.2480089](https://doi.org/10.1109/TED.2015.2480089).
- [24] H. T. Hsueh, Y. J. Hsiao, Y. D. Lin and C. L. Wu, "Bifacial Structures of ZnS Humidity Sensor and Cd-Free CIGS Photovoltaic Cell as a Self-Powered Device," in *IEEE Electron Device Letters*, vol. 35, no. 12, pp. 1272-1274, Dec. 2014, doi: [10.1109/LED.2014.2361648](https://doi.org/10.1109/LED.2014.2361648).
- [25] J. A. Ruiz-Arias, E. F. Fernández, Á. Linares-Rodríguez and F. Almonacid, "Analysis of the Spatiotemporal Characteristics of High Concentrator Photovoltaics Energy Yield and Performance Ratio," in *IEEE Journal of Photovoltaics*, vol. 7, no. 1, pp. 359-366, Jan. 2017, doi: [10.1109/JPHOTOV.2016.2623089](https://doi.org/10.1109/JPHOTOV.2016.2623089).
- [26] M. Schweiger, W. Herrmann, A. Gerber and U. Rau, "Understanding the energy yield of photovoltaic modules in different climates by linear performance loss analysis of the module performance ratio," in *IET Renewable Power Generation*, vol. 11, no. 5, pp. 558-565, 12 4 2017, doi: [10.1049/iet-rpg.2016.0682](https://doi.org/10.1049/iet-rpg.2016.0682).



Mahmoud Dhimish is Lecturer in Electronics and Control Engineering at the University of Huddersfield, UK. He graduated with MSc. in Electronic and Communication Engineering (Distinction) from the University of Huddersfield. Following this he gained a Ph.D. in Renewable Energy. His research interests include design, control, reliability, and performance analysis of photovoltaic

systems using novel mathematical, statistical, and probabilistic modeling techniques. His current research focuses on analysing the impact of hot-spots on performance of PV systems.



Peter Mather is a senior lecturer at School of Computing and Engineering, University of Huddersfield. He is the course leader for all the MEng/BEng & BSc electronics courses. He is currently developing a wide range of electronic and associated systems from VHDL/FPGA development to Sigma-Delta ADC testing of mixed signal devices. He also investigating integrated sustainable energy networks in order to optimize

commercial and domestic energy usage within existing premises.



Violeta Holmes is a Subject Area Leader for Electronic and Electrical Engineering at the Huddersfield University with over 25 years of teaching and research experience in computing and engineering. She leads the High Performance Computing (HPC) Research Group at the University of Huddersfield. Her research interests and expertise are in the areas of HPC systems infrastructure, Internet of Things and

Embedded Systems.